EUROPEAN FUSION DEVELOPMENT AGREEMENT

EFDA–JET–CP(04)07-47

C. Sozzi, E. Minardi, E. Lazzaro, S. Cirant, B. Esposito, F. Imbeaux, P. Mantica, M. Marinucci, M. Romanelli and JET EFDA Contributors

Experimental Observations Related to the Thermodynamic Properties of Tokamak Plasmas

Experimental Observations Related to the Thermodynamic Properties of Tokamak Plasmas

C. Sozzi[1], E. Minardi[1], E. Lazzaro[1], S. Cirant[1], B. Esposito[2], F. Imbeaux[3], P. Mantica[1], M. Marinucci[1], M. Romanelli[2] and JET EFDA Contributors*

[1]Istituto di Fisica del Plasma, CNR – Associazione Euratom-ENEA-CNR, Milano, Italia
[2]Associazione Euratom-ENEA, Frascati, Italia
[3]Association Euratom-CEA, Cadarache, France
** See annex of J. Pamela et al, "Overview of JET Results ", (Proc.20 [th] IAEA Fusion Energy Conference, Vilamoura, Portugal (2004).*

Preprint of Paper to be submitted for publication in Proceedings of the
20th IAEA Conference,
(Vilamoura, Portugal 1-6 November 2004)

ABSTRACT.
The coarse-grained tokamak plasma description derived from the magnetic entropy concept presents appealing features as it involves a simple mathematics and it identifies a limited set of characteristic parameters of the macroscopic equilibrium. In this paper a comprehensive review of the work done in order to check the reliability of the Stationary Magnetic Entropy predictions against experimental data collected from different tokamaks, plasma regimes and heating methods is reported.

1. INTRODUCTION.

A great effort has been devoted for many years in the magnetic confinement community performing both aimed experiments and theoretical work in order to come out physics based models of the fusion plasma. The present understanding indicates that the most satisfactory and effective description of the plasma in reactor relevant conditions should assume as starting point the detailed dynamics of the particles and of the fields and their collective behaviour including microscopic instabilities and turbulence. However, the enormous complexity of the task could suggest that insights coming from complementary global approaches are useful as well, as much as their basic assumptions are physically meaningful and widely applicable.

In this frame, the coarse-grained tokamak plasma description derived from the magnetic entropy concept [1] presents appealing features as it involves a simple mathematics and it identifies a limited set of characteristic parameters of the macroscopic magnetic equilibrium. The capability of the SME analysis to describe tokamak plasma profiles in Ohmic and L mode with relevant additional heating has been reported in previous papers [3-5]. In the case of the tokamak, which is an open system, the magnetic entropy takes the form of a stationary functional, expressing the balance between entropy injected and produced in the system (SME, Stationary Magnetic Entropy). The SME condition is given by the following equation for the current density profile

$$\nabla^2 \vec{j} + \mu^2 \vec{j} = -\frac{\mu^2}{E}(p_A - p_L) \qquad (1)$$

where E is the toroidal electric field, m is a parameter of the theory and the density distributions of additional power sources and non diffusive losses for the electron population are described by p_A, p_L respectively. Moreover, other verifiable predictions result from the requirements of consistency with the Grad-Shafranov equation and with the power balance equation, giving restrictive constraints to the electron pressure profile and to the electron heat flux profile respectively [3-4].

A key point is that the electron heat flux can be related to the heating sources through the solution of the equation (1) and is therefore entirely determined by the magnetic configuration through the condition of stationary entropy. In situations where the auxiliary heating is dominant with respect to the Ohmic heating equation (1) is invariant when the combination $m^2 p_A / E$ of the parameters does not change, a feature that gives rise to the profile consistency.

The natural field of application of the theory concerns relaxed states in which the dissipation

processes are counterbalanced by external sources (Ohmic or auxiliary) such that the magnetic entropy and the plasma state are constant in time. Nevertheless it is worthwhile to check the validity of the theory in a variety of situations in order to gain comprehensive view of its limits of validity.

The aim of this paper is to provide such a view comparing the SME predictions with experimental data collected from different tokamaks, plasma regimes and heating methods. In particular the capability of the theory to give a reliable description of the tokamak plasma profiles under a limited number of assumptions, taken from experimental data or testable a posteriori is discussed. The role of the m parameter and its relationship with the experimental quantities is analysed in the paper as well.

2. DATABASE AND METHOD OF ANALYSIS

This paper complements previous tokamak profile analysis performed with the SME method on FTU and JET plasmas with additional heating, limited to magnetic configurations in which the safety factor at the plasma centre was lower than one [4-5]. The analysis of non monotonic safety factor profiles with q>1 everywhere was possible solving equation (1) with the appropriate boundary conditions discussed in [2]. The present analysis based on the generalized SME equation (2) is focused on q>1 plasmas although includes for comparison $q_0<1$, L mode plasmas. The shot analysed are listed in Table I, along with the main plasma parameter and heating systems.

Different heating scenarios have been included in the analysis, from highly localized EC heated plasmas of TS and AUG to broader electron heating obtained in JET using the Mode Conversion ICRF. The effects of high magnetic field (7.2 T) and high electron density have been explored in a set of Ohmic shots of FTU at different plasma currents (0.5-1.4MA). The effect of the plasma elongation have been explored comparing quasi circular plasmas of FTU and TS with elongated plasmas of JET and AUG. A number of different plasma scenarios and confinement regimes have been explored as well, studying L mode of FTU, TS, AUG and JET and H mode, ITB and Hybrid Mode scenarios of JET.

In order to take into account the boundary conditions on axis, where $q \geq 1$, eq.(1) is more conveniently written in the form

$$\nabla^2 y(x) + \mu(x)^2 \, y(x) + \mu(x)^2 \, (p_A - p_L) = 0 \qquad (2)$$

where $y = Ej(x)$ and $m(x))$ is now a two valued complex step function of the radial coordinate x:

$$\mu(x) = i\mu_1 \quad x < \xi; \quad \mu(x) = \mu_2 \; x > \xi \qquad (3)$$

Here m1, m2,x . are chosen in order that $y(x)$ be continous in x with its first derivative, consistently with the boundary conditions on axis and at the border. The coordinate x is normalized to the width of the so called confinement region, dominated by diffusive transport, extending from the plasma center to the radius in which the edge effects are relevant and radiation losses increase. In the analysis the external border of the confinement region has been usually assumed equal to 0.75 r/a.

The first step of the analysis consists in a standard interpretative transport simulation performed with a power balance code (JETTO, ASTRA, CRONOS, EVITA), using for the input profiles the experimental data, including, for part of the JET shots, the safety factor benchmarked with the Motional Stark Effect. This process produces the radial profiles of the current density and of the ion temperature (if not directly measured), the heat flux and the effective electron diffusivity. The second step consists in the calculation of the plasma profiles accordingly to the SME theory, starting from the input of the additional power density, of the plasma density and of a few global plasma parameters (toroidal magnetic field B, plasma current I_p, effective ion charge Z_{eff}). The model is implemented in a code in which the three values describing the step function m(x) are free parameters. These parameters are adjusted to the experimental boundary conditions until the calculated profiles reproduce the experimental ones (whenever this is possible) minimising a figure of merit introduced in order to give a quantitative evaluation of the simulation. For a given physical quantity F function of the radial coordinate (e.g., the electron temperature) the figure of merit F_{err} is

$$F_{err} = \sqrt{\frac{\Sigma(F_{i,SME} - F_{i,EXP})^2}{\Sigma F_{i,EXP}^{\ 2}}} \qquad (4)$$

where $F_{i,SME}$ and $F_{i,EXP}$ are respectively the calculated and experimental data points at the radii x_i. The analysis has been focused on four quantities: the safety factor $q(x)$, the electron temperature $T_e(x)$, the heat flux $Q(x)$ and the loop voltage$V = 2\pi RE$,where R is the major radius of the tokamak. It is important to note here that the SME equation actually provides restrictive conditions on the pressure profile, in particular the pressure profile is essentially determined by its zero order moment once the poloidal magnetic configuration is known. However, in the present analysis the comparison with the calculated temperature is appropriate, being the density taken from experiments. On the other hand, for testing the energy transport, the comparison with the heat flux rather than with effective electron diffusivity has been preferred, in view of its more global character with respect to the generally strong dependence of the diffusivity on local gradients. Moreover, the heat flux is a true figure of merit for the SME equation, being strictly dependent on the magnetic configuration and not on the temperature profile that can be obtained only introducing additional hypothesis like ohmic relaxation.

3. RESULTS AND DISCUSSION

The results of the present analysis are summarized in Table II, which includes the values of the free parameter in the equation (2) and the figures of merit for the main quantities related to the SME. In most of the cases the safety factor profile is reasonably well reproduced (q_{err}<<1). This observation is particularly significant when the figure of merit for the loop voltage *Verr* (defined by equation (4) for i=1) is much less than 1. Indeed the loop voltage is determined through the $m^2 p_A / E$ invariance of the SME equation that poses severe constraints to the combination of the free parameters m_1, m_2,x .

In general, when the assumption of Ohmic relaxation is little or not at all verified as in presence of internal or external transport barriers the figures of merit Q_{err} and T_{err} are not satisfactory. In these cases the general behaviour of the heat flux profile calculated in accordance with SME is often still comparable with the experimental data, but the calculated electron temperature is generally not satisfactory. This is shown for example in the comparison between FIG. 1 (shot 58148) and FIG.2 (shot 56083) for the H mode plasma of JET. The safety factor profile is well described all across the confinement region in both the cases, but the calculated electron temperature is in good agreement with the experiment only in the external region for the 58148 case. A similar situation is presented in the FIG. 3, showing the results for the electron ITB plasma 53506 of JET. In this case the electron temperature is well described outside of the barrier region. The heat flux $Q(x)$ miss the spatial details, but still follows the general behaviour of the experiment. FIG. 4 shows the simulation of the full non inductive plasma 30007 of TS, where the whole current I_p=0.66 MA is sustained by radiofrequency injection, and then the resistive link between current density and temperature is broken. In this case of course the SME analysis fails to produce the correct temperature profile, still the heat flux is in surprising agreement with the experimental data. This fact support the link between heat transport and magnetic configuration implied in the SME equation (1), which is basically a power balance equation [1,4]. FIG.5 shows the correspondence with the experimental data of the local effective diffusivity derived from the SME theory [4] using the experimental electron temperature profile instead of the Ohmic relaxation one.

CONCLUSIONS

The SME analysis so far performed provides a satisfactory description of the safety factor profile (directly related to the current density derived from eq.(2)) in all machines and in the L and H confinement modes and also of the temperature profile whenever Ohmic relaxation $T_e \mu j^{2/3}$ can be assumed.

In these cases the restrictions on the pressure profile provided by the SME theory are consistent with the experiments, showing that the normalised experimental pressure can be reasonably reproduced assuming its zero order moment only.

Preliminary results obtained in advanced tokamak scenarios indicate a similar capability in the reproduction of the q profile. However in the presence of H modes, ITB or strong non inductive current drive the comparison of the electron temperature profile with the predictions of SME is not satisfactory. The agreement found in many cases between the heat flux derived from the SME equation and the experimental heat flux seems to indicate a general fact which however needs further confirmation.

REFERENCES

[1]. E.Minardi, J. Plasma Phys. **70**, 2004, Part 6

[2]. E. Lazzaro and E. Minardi J. Plasma Phys. **63**, 2001, 1

[3]. E.Minardi and H.Weisen, Nuclear Fusion **41**,2001,113

[4]. E.Minardi, E.Lazzaro, C.Sozzi, S.Cirant, Nuclear Fusion **43**, 2003, 369

[5]. C.Sozzi, E.Minardi, E.Lazzaro, P.Mantica and JET EFDA Contributors, 30th EPS Conf. on Plasma Phys. Contr. Fusion, S.Petersburg, Russia, 7-11-July 2003, Paper P.1.94.

MAC	SHOT	Regime	I_p (MA)	n_{e0} (10^{20})	B_0 (T)	Elong.	P_{add}	Main Heating
JET	59397	ITB	2.8	0.33	3.45	1.69	17	NBI+ICRH
JET	62077	ITB	2.6	0.31	3.2	1.46	20	NBI+ICRH
JET	53506	e-ITB	2.4	0.16	3.4	1.49	6	ICRH+LH
JET	53521	ITB	2	0.51	3.4	1.515	22	NBI+ICRH
JET	56083	H	2.5	1.15	2.7	1.595	15	NBI+ICRH
JET	59211	H	1.8	0.53	2.8	1.37	12	NBI
JET	53822	L	1.9	0.35	3.4	1.45	6	ICRH
JET	58148	H	1.8	0.29	3.4	1.575	18	NBI+ICRH
JET	62789	Hyb	2.6	0.32	3.2	1.465	20	ICRH+NBI
JET	53298	H	2.5	0.56	2.6	1.54	15	NBI
JET	44013	H	2.5	0.68	2.7	1.575	15	NBI
JET	62608	ITB	2.5	0.28	3.4	1.55	9	ICRH+NBI
AUG	17175	L	0.4	0.27	2.05	1.595	1.5	ECRH
AUG	16978	L	0.4	0.35	2.1	1.695	1.5	ECRH
TS	31165	L	1	0.33	3.865	1.025	0	OHMIC
TS	31165	L	1	0.36	3.865	1.025	0.8	ECRH
TS	30555	L	1	0.22	3.84	1.025	0.8	ECRH
TS	30007	L (full CD)	0.66	0.23	3.84	1.025	3	LHCD
FTU	23159	L	0.5	0.6	7.2	1.03	0	OHMIC
FTU	23053	L	1.1	1	7.2	1.026	0	OHMIC
FTU	23179	L	1.4	2.59	7.2	1.026	0	OHMIC

JG05.105-1c

TABLE I: List of analysed shots

MAC	SHOT	μ_1	μ_2	ξ	Q_{err}	q_{err}	T_{err}	V_{err}
JET	59397	0.165	0.74	0.3	0.823	0.295	0.216	0.695
JET	62077	3.214i	0.714	0.15	0.26	0.117	0.185	0.259
JET	53506	1.312	1.312	0.15	0.443	0.181	0.556	0.146
JET	53521	0.473	0.473	0.23	0.243	0.413	0.683	0.03
JET	56083	−1.5i	1	0.5	0.6	0.047	0.163	0.553
JET	59211	−1	0.9	0.08	7.261	0.093	0.555	3.38
JET	53822	−6.522i	0.595	0.08	0.904	0.083	0.154	0.297
JET	58148	−0.833i	0.643	0.08	0.319	0.07	0.198	0.968
JET	62789	−0.49i	1.35	0.1	0.467	0.058	0.678	2.2759
JET	53298	−1	0.9	0.08	2.131	0.056	0.587	4.022
JET	44013	−i	0.8	0.5	0.935	0.037	0.194	1.272
JET	62608	1.9	1.5	0.15	0.643	0.173	0.441	0.458
AUG	17175	2.25	0.2	0.76	1.024	0.167	0.218	0.805
AUG	16978	2.2i	0.8	0.65	1.942	0.192	0.127	2.239
TS	31165	0.8i	5	0.17	0.511	0.205	0.153	0.307
TS	31165	1.8	2.3	0.405	0.479	0.216	0.168	0.487
TS	30555	−6.21	0.6	0.15	35.223	0.11	0.845	8.42
TS	30007	0.55	0.28	0.12	0.143	0.255	0.82	48.8
FTU	23159	14i	0.85	0.06	1.903	0.134	0.17	0.217
FTU	23053	15.5i	0.85	0.055	8.164	0.087	0.408	0.144
FTU	23179	16.667i	0.85	0.055	4.4675	0.137	0.478	0.475

JG05.105-2c

TABLE II: Summary of the analyis results

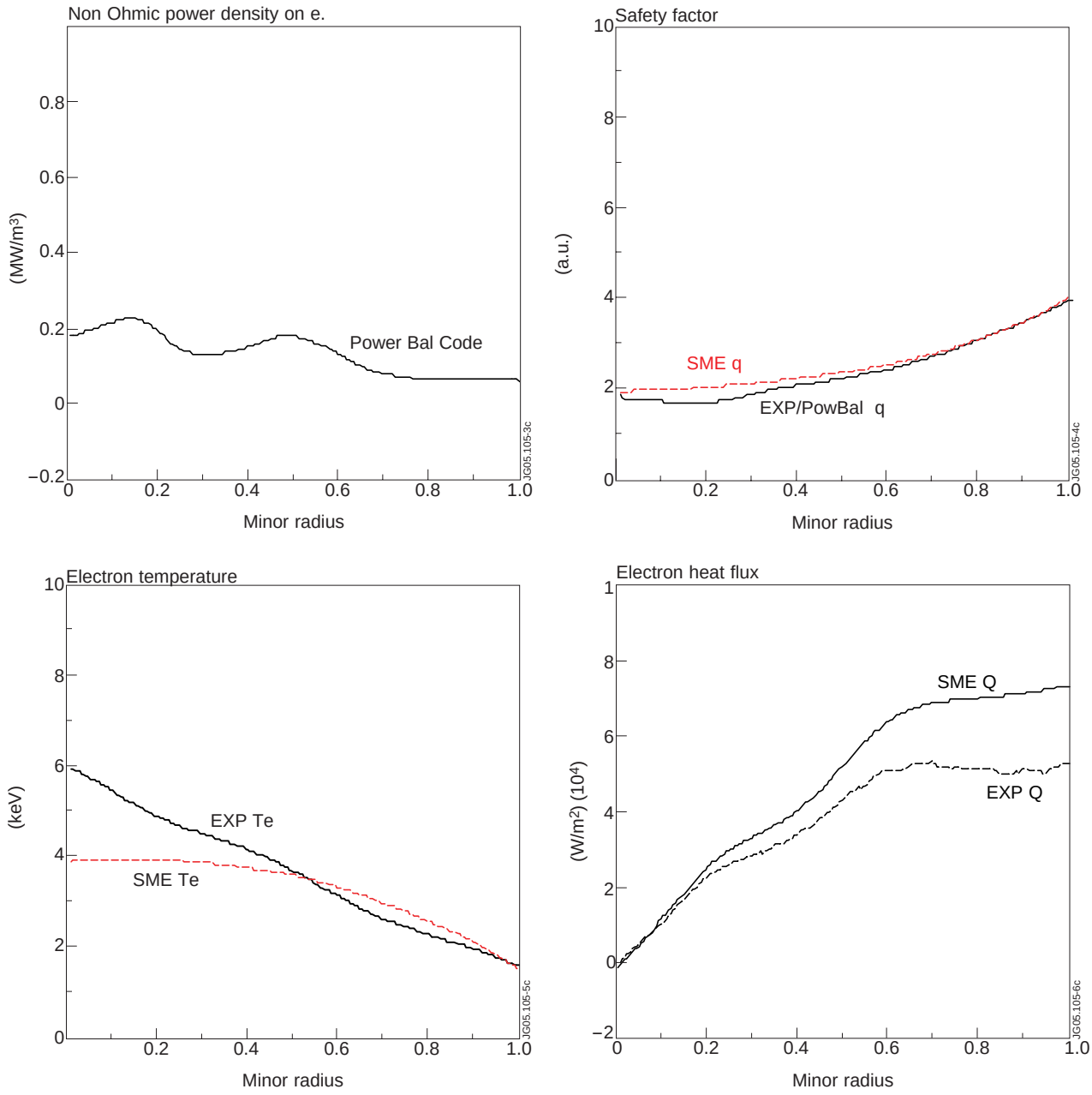

Figure 1: H mode JET Pulse No: 58148

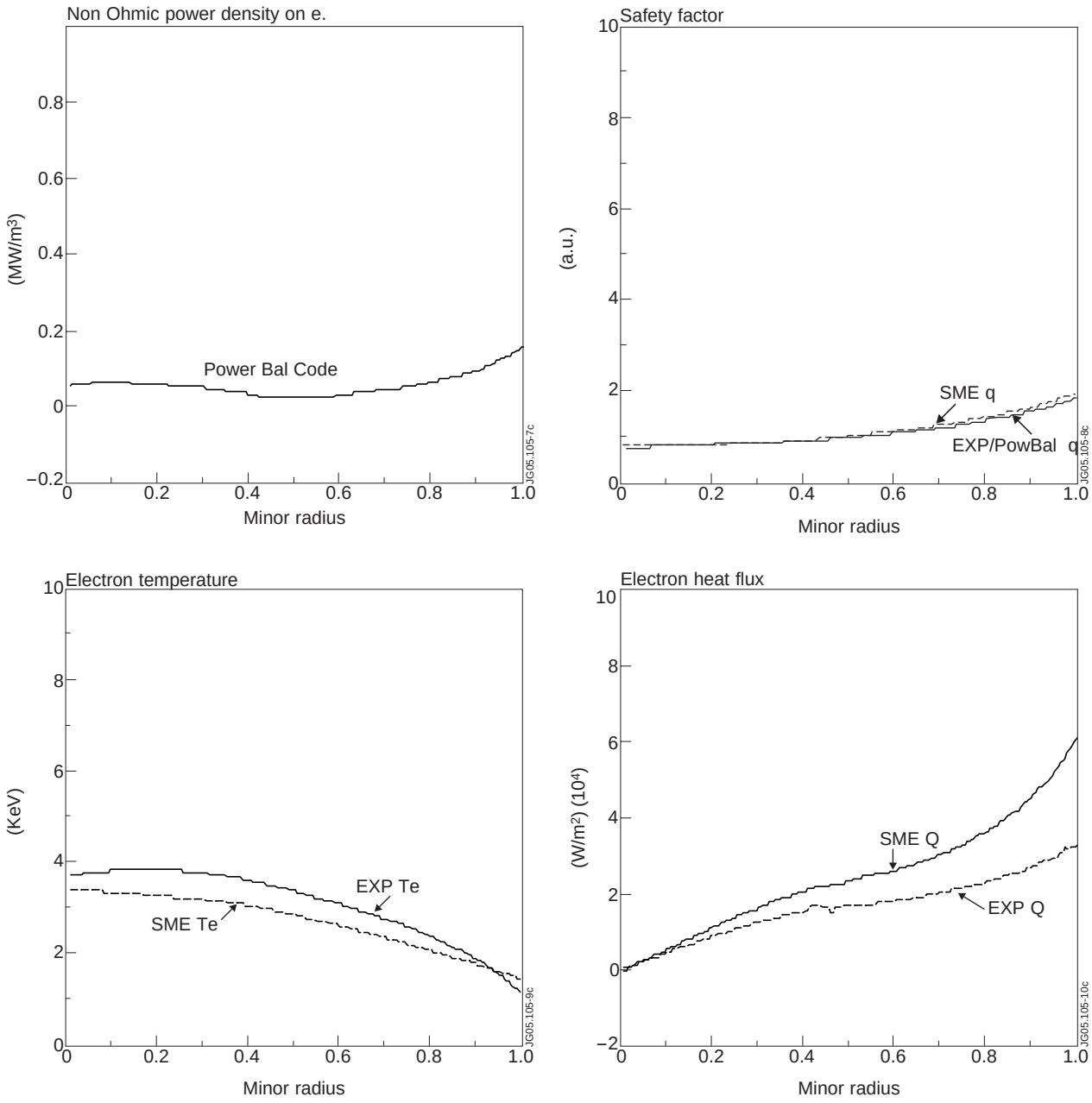

Figure 2: H mode JET Pulse No: 56083

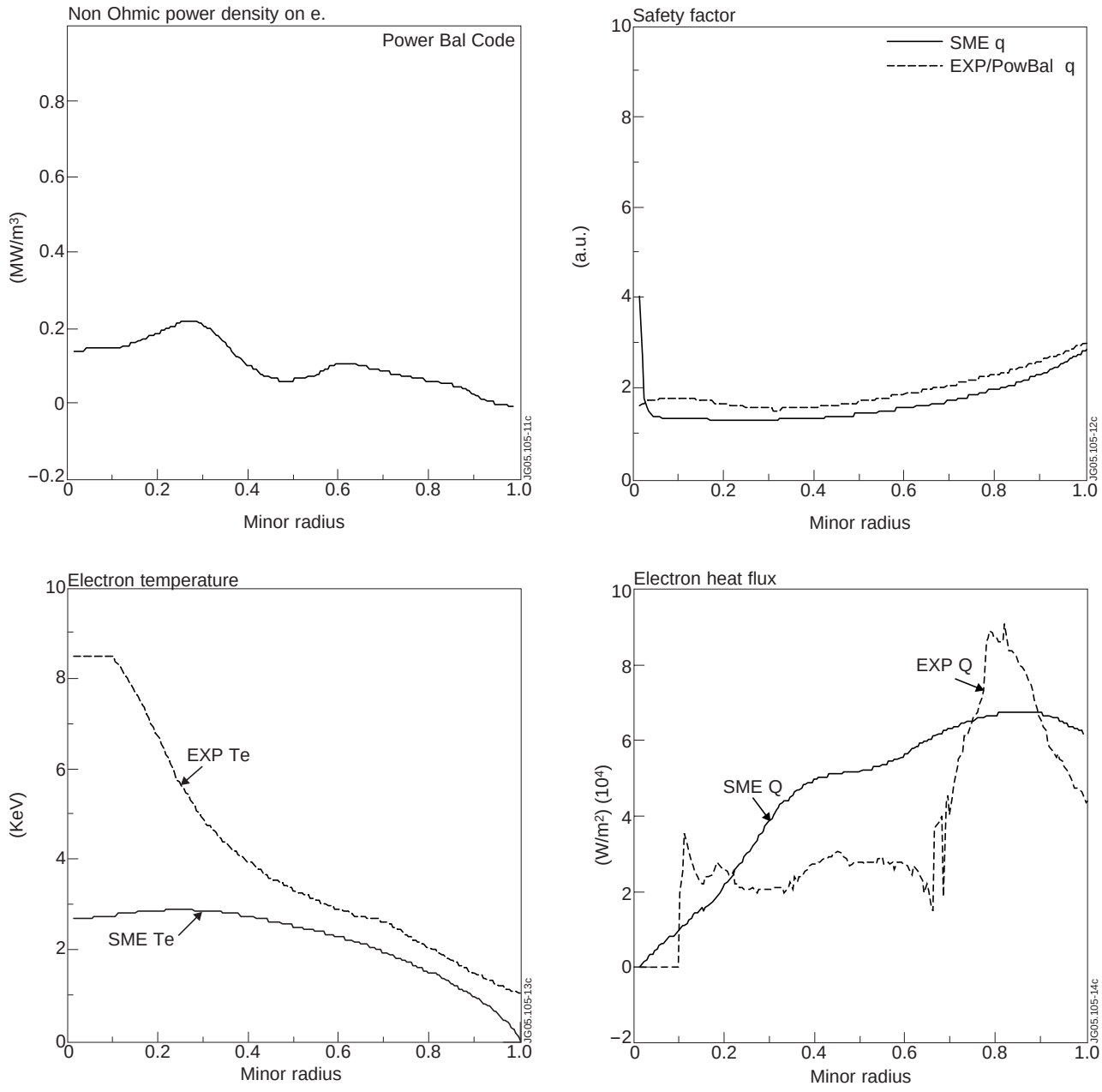

Figure 3: Electron ITB JET Pulse No: 53506

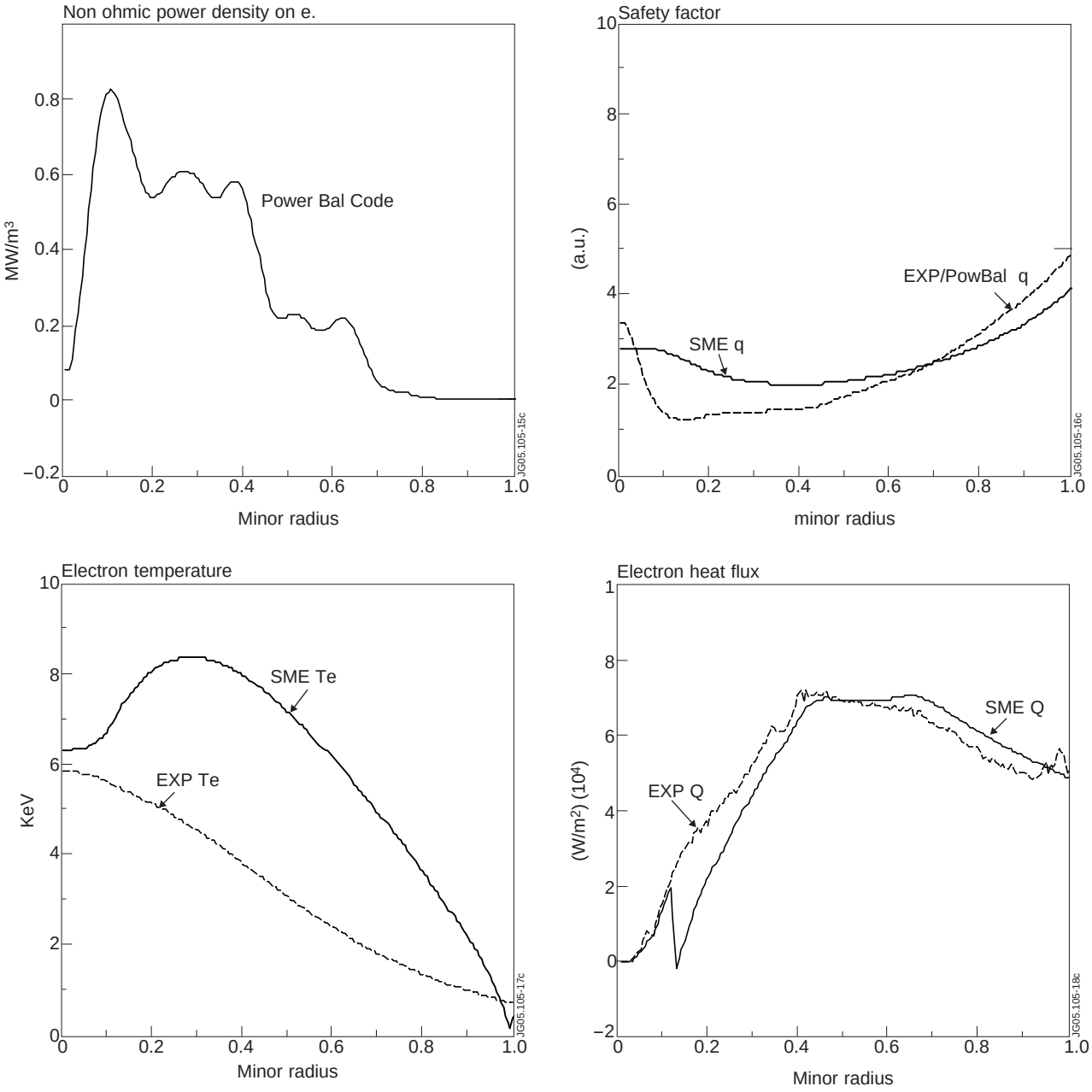

Figure 4: Full current drive JTS 30007

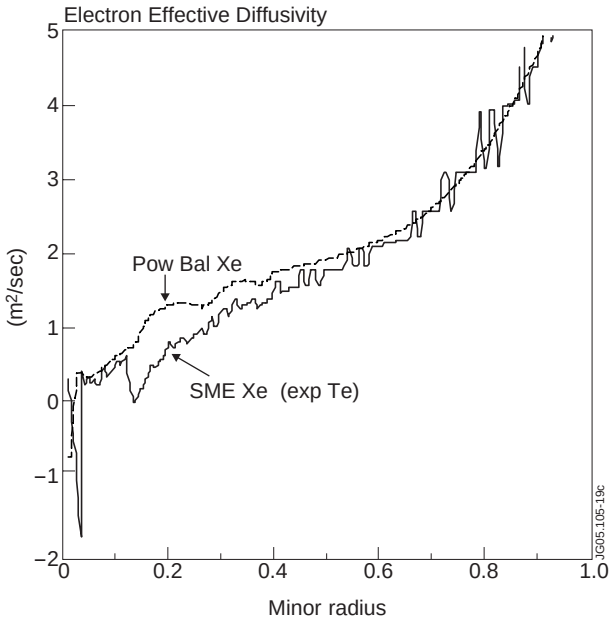

Figure 5: Effective diffusivity TS 30007